JOC Article

Design and Development of a New Pyrromethene Dye with Improved Photostability and Lasing Efficiency: Theoretical Rationalization of Photophysical and Photochemical Properties

Soumyaditya Mula,[†] Alok K. Ray,[‡] Manas Banerjee,[§] Tandrima Chaudhuri,[§] Kamalesh Dasgupta,[‡] and Subrata Chattopadhyay*[,†]

Bio-Organic Division, Laser and Plasma Technology Division, Bhabha Atomic Research Centre, Mumbai - 400085, India, and Chemistry Department, Burdwan University, Burdwan - 713104, India

schatt@barc.gov.in

Received October 31, 2007

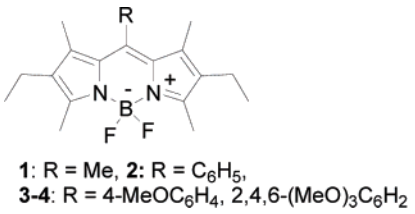

In an attempt to develop a photostable and efficient pyrromethene compound for use in liquid dye lasers, three congeners of the commercially available pyrromethene 567 (PM567) laser dye were synthesized and their photophysical properties, lasing efficiencies, and photochemical stabilities were studied. In general the presence of an aryl group at C-8 of the pyrromethene chromophore increased the photostability. One of the congeners possessing a C-8 trimethoxyphenyl moiety showed significantly improved lasing parameters than PM567. Compared to PM567, the photochemical stability of the new dye was 2-fold, while it showed an equivalent lasing efficiency to that of PM567 at a significantly lower concentration. The increased photostability of these new dye molecules could be explained by theoretical calculation on their capacity to generate singlet oxygen ($^1O_2$) and probability of reaction with $^1O_2$. Our calculations were in agreement with the experimental results and indicated that a systematic design of new derivatives of pyrromethene chromophore might lead to improved laser dye molecules.

Introduction

Dipyrromethene-BF_2 (PM) fluorophores (4,4-difluoro-4-bora-3a,4a-diaza-s-indacene) (Figure 1) are highly fluorescent dyes and used for such diverse applications as biolabels,[1a] artificial light harvesters,[1b] sensitizers for solar cells,[1c] fluorescent sensors,[1d−k] molecular photonic wires,[1l,m] and electron-transfer reagents.[1n] Further, these dyes are also very useful for laser applications since they have a low intersystem crossing (ISC) rate and low triplet excitation coefficients over the laser spectral region[2a−f] and often possess a triplet−triplet absorption coefficient about one-fifth that of the rhodamine dyes.[3a,b] These are ionic dyes exhibiting good solubility in many organic solvents and even in methyl methacrylate (MMA) that is useful for solid-state dye laser applications.[4a−d] Some of the PM dyes outperform the widely used laser dye, rhodamine 6G (Rh6G), considered as the benchmark in lasing efficiency and photochemical stability. The two major inherent deficiencies of the PM dyes are their small Stokes' shift and photochemical instability. The former reduces the lasing efficiency of the PM dyes due to the ground state absorption (GSA). The problem has been partially

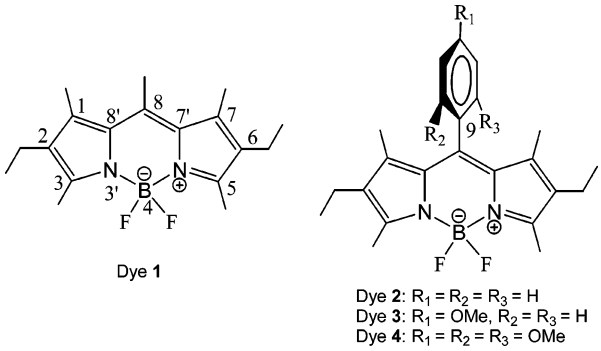

FIGURE 1. Chemical structures of the PM dyes **1**−**4**.

* Fax: 91-22-5505151.
† Bio-Organic Division, Bhabha Atomic Research Centre.
‡ Laser and Plasma Technology Division, Bhabha Atomic Research Centre.
§ Burdwan University.

10.1021/jo702346s CCC: $40.75
Published on Web 02/27/2008

SCHEME 1[a]

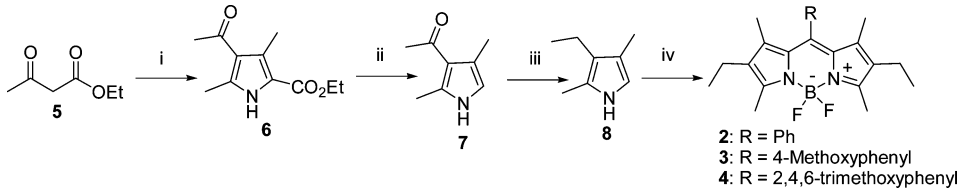

[a] (i) (a) $NaNO_2/CH_3CO_2H$/15 °C/overnight; (b) Acetylacetone/Zn/60 °C/1 h, (ii) KOH/ethylene glycol/160 °C/4 h, (iii) $LiAlH_4$/THF/Δ/4.5 h, (iv) (a) RCHO/4-toluenesulphonic acid/CH_2Cl_2/25 °C/24 h; (b) DDQ/4 h; (c) Et_3N/1 h; (d) $BF_3{\cdot}Et_2O$/25 °C/4 h.

resolved by incorporating simple or bicyclic rigid aryl substituents at the C-3 center or the boron atom of the PM moiety.[5a−d] Although the lasing action of the PM dyes has been the primary focus of research,[6a] more effort is needed to enhance their photostability, especially for commercial applications. The photodegradation of the PM dyes is mediated by their photochemical reaction with singlet oxygen.[6b,c] Some solid-state dye laser materials containing dispersed PM dyes, developed with the primary aim of improving the laser energy output,[4b−e] also showed better photostability compared to liquid dye lasers. Possibly, polymerization of the suitable monomer containing the dispersed dyes provides the polymeric solid matrix free of oxygen, increasing the photochemical half-lives of dyes. However, the photochemical degradation continues to be a hurdle in the long-term operation of the PM-based liquid dye lasers, especially for high power and high-repetition rate operation.[7a,b]

It was envisaged that suitable modifications of the substitution pattern of the PM dyes might provide a photostable laser dye with better spectral and lasing properties. Earlier, similar approaches have been adopted to synthesize a host of analogues of the most extensively used laser dye, PM567 (**1**), by incorporating different substituents at C-8 and/or C-2 + C-6 positions of the pyrromethene moiety.[2a,6c,d] Among these, PM650 (with a C-8 CN) showed a ∼50 times higher half-life than **1**.[6c] In contrast, the effect of alteration of the alkyl substituents at the pyrrole rings was much less.[6d] Most importantly, the fluoresecence quantum yields of these analogues were too low to be used as laser dyes.[2a,6c] It was felt that a systematic study on this aspect to improve the photochemical stabilities of the PM dyes in solution is lacking. The primary aim of the investigation was to develop a photostable and efficient laser dye by rational design. To this end, we considered **1** as the model reference dye, synthesized its three congeners **2**−**4**, studied their lasing property and photostability, and rationalized the results in terms of their photophysical and photochemical attributes as well as theoretical calculations.

Results and Discussion

It is now well established[6b−d] that the triplet state of the excited PM dye molecules generates singlet oxygen ($^1O_2$), which reacts primarily at the C-7′−C-8 double bond of the dye molecules. This produces an unstable peroxo compound, eventually leading to the breakdown of the dye structure. The involvement of the triplet state of the dyes in the process was revealed from their fast decomposition in the presence of a triplet sensitizer, like benzophenone (BP).[6c] Likewise, the enhanced operating life of the deoxygenated dye solutions,[4d] and also in the presence of 1 wt % of singlet oxygen quenchers, such as Tin770, TBP,[6d] and especially DABCO,[3b,6b] confirmed the participation of $^1O_2$ in the dye degradation.

Thus, the photostability of the PM dyes might be increased by reducing or eliminating their reaction with $^1O_2$ and/or reducing generation of $^1O_2$. It was anticipated that steric

(1) (a) Haugland, R. P. *Handbook of Fluorescent Probes and Research Chemicals*, 6th ed.; Molecular Probes: Eugene, OR, 1996. (b) Lokey, G. E.; Hanes, M. S.; Bailey, S. T.; Shearer, J. D. M.; Zhang, Y.-Z.; Wittmershaus, B. P. Presented at the 225th ACS National Meeting, New Orleans, LA, March 23−27, 2003. (c) Hattori, S.; Ohkubo, K.; Urano, Y.; Sunahara, H.; Nagano, T.; Wada, Y.; Tkachenko, N. V.; Lemmetyinen, H.; Fukuzumi, S. *J. Phys. Chem. B* **2005**, *109*, 15368−15375. (d) Rurack, K.; Kollmannsberger, M.; Resch-Genger, U.; Daub, J. *J. Am. Chem. Soc.* **2000**, *122*, 968−969. (e) Turfan, B.; Akkaya, E. U. *Org. Lett.* **2002**, *4*, 2857−2859. (f) Goze, C.; Ulrich, G.; Charbonnière, L.; Cesario, M.; Prange', T.; Ziessel, R. *Chem.—Eur. J.* **2003**, *9*, 3748−3755. (g) Gabe, Y.; Urano, Y.; Kikuchi, K.; Kojima, H.; Nagano, T. *J. Am. Chem. Soc.* **2004**, *126*, 3357−3367. (h) Yogo, T.; Urano, Y.; Ishitsuka, Y.; Maniwa, F.; Nagano, T. *J. Am. Chem. Soc.* **2005**, *127*, 12162−12163. (i) Ueno, T.; Urano, Y.; Kojima, H.; Nagano, T. *J. Am. Chem. Soc.* **2006**, *128*, 10640 -10641. (j) Oleynik, P.; Ishihara, Y.; Cosa, G. *J. Am. Chem. Soc.* **2007**, *129*, 1842−1843. (k) Sunahara, H.; Urano, Y.; Kojima, H.; Nagano, T. *J. Am. Chem. Soc.* **2007**, *129*, 5597−5604. (l) Wagner, R. W.; Lindsey, J. S. *J. Am. Chem. Soc.* **1994**, *116*, 9759−9760. (m) Li, F.; Yang, S. I.; Ciringh, Y.; Seth, J.; Martin, C. H.; Singh, D. L.; Kim, D.; Birge, R. R.; Bocian, D. F.; Holten, D.; Lindsey, J. S. *J. Am. Chem. Soc.* **1998**, *120*, 10001−10017. (n) Debreczeny, M. P.; Svec, W. A.; Wasielewski, M. R. *Science* **1996**, *274*, 584−587.

(2) (a) Pavlopoulos, T.; Boyer, J. H.; Shah, M.; Thangaraj, K.; Soong, M. L. *Appl. Opt.* **1990**, *29*, 3885−3889. (b) Pavlopoulos, T.; Boyer, J. H.; Thangaraj, K.; Sathyamoorthi, G.; Shah, M. P.; Soong, M. L. *Appl. Opt.* **1992**, *31*, 7089−7094. (c) Guggenheimer, S. C.; Boyer, J. H.; Thangaraj, K.; Shah, M. P.; Soong, M. L.; Pavlopoulos, T. *Appl. Opt.* **1993**, *32*, 3942−3943. (d) Boyer, J. H.; Haag, A. M.; Satyamoorthi, G.; Soong, M. L.; Thangaraj, K.; Pavlopoulos, T. *Heteroat. Chem.* **1993**, *4*, 39−49. (e) Ricardo, D.; Lucia, B. S.; Angel, C.; Inmaculada, G. M.; Roberto, S.; Alberto, U. A. *Appl. Opt.* **2003**, *42*, 1029−1035. (f) Pavlopoulos, T. G.; Shah, M.; Boyer, J. H. *Opt. Commun.* **1989**, *70*, 425−427.

(3) (a) O'Neil, M. P. *Opt. Lett.* **1993**, *18*, 37−38. (b) Pavlopoulos, T.; Boyer, J. H. *Proc. SPIE- Int. Soc. Opt. Eng.* **1994**, *2115*, 231−239.

(4) (a) Faloss, M.; Canva, M.; Georges, P.; Brun, A.; Chaput, F.; Boilot, J. *Appl. Opt.* **1997**, *36*, 6760−6763. (b) Costela, A.; Garcia-Moreno, L.; Sastre, R. *Phys. Chem. Chem. Phys.* **2003**, *5*, 4745−4763. (c) Ray, A. K.; Kumar, S.; Mayekar, N. V.; Sinha, S.; Kundu, S.; Chattopadhyay, S.; Dasgupta, K. *Appl. Opt.* **2005**, *44*, 7814−7822. (d) Turro, N. J. *Modern Molecular Photochemistry*; University Science Books: CA, 1991; p 588. (e) Arbeloa, F. L.; Prieto, J. B.; Arbeloa, I. L.; Costela, A.; Garcia-Moreno, I.; Gomez, C.; Amat-Guerri, F.; Liras, M.; Sastre, R. *Photochem. Photobiol.* **2003**, *78*, 30−36.

(5) (a) Burghart, A.; Kim., H.; Welch, M. B.; Thoresen, L. H.; Reibenspies, J.; Burgess, K. *J. Org. Chem.* **1999**, *64*, 7813−7819. (b) Chen, J.; Burghart, A.; Derecskei-Kovacs, A.; Burgess, K. *J. Org. Chem.* **2000**, *65*, 2900−2906. (c) Harriman, A.; Izzet, G.; Ziessel, R. *J. Am. Chem. Soc.* **2006**, *128*, 10868−10875. (d) Goze, C.; Ulrich, G.; Mallon, L. J.; Allen, B. D.; Harriman, A.; Ziessel, R. *J. Am. Chem. Soc.* **2006**, *128* 10231−10239.

(6) (a) Rahn, M. D.; King, T. A.; Gorman, A. A.; Hamblett, I. *Appl. Opt.* **1997**, *36*, 5862−5871. (b) Rahn, M. D.; King, T. A. *Appl. Opt.* **1995**, *34*, 8260−8271. (c) Jones, G. H.; Klueva, O.; Kumar, S.; Pacheco, D. *Solid State Lasers SPIE* **2001**, *24*, 4267−4271. (d) Jones, G., II; Kumar, S.; Klueva, O.; Pacheco, D. *J. Phys. Chem. A* **2003**, *107*, 8429−8434.

(7) (a) Assor, Y.; Burshtein, Z.; Rosenwaks, S. *Appl. Opt.* **1998**, *37*, 4914−4920. (b) Ray, A. K.; Kundu, S.; Sasikumar, S.; Rao, C. S.; Mula, S.; Sinha, S.; Dasgupta, K. *Appl. Phys. B* **2007**, *87*, 483−488.

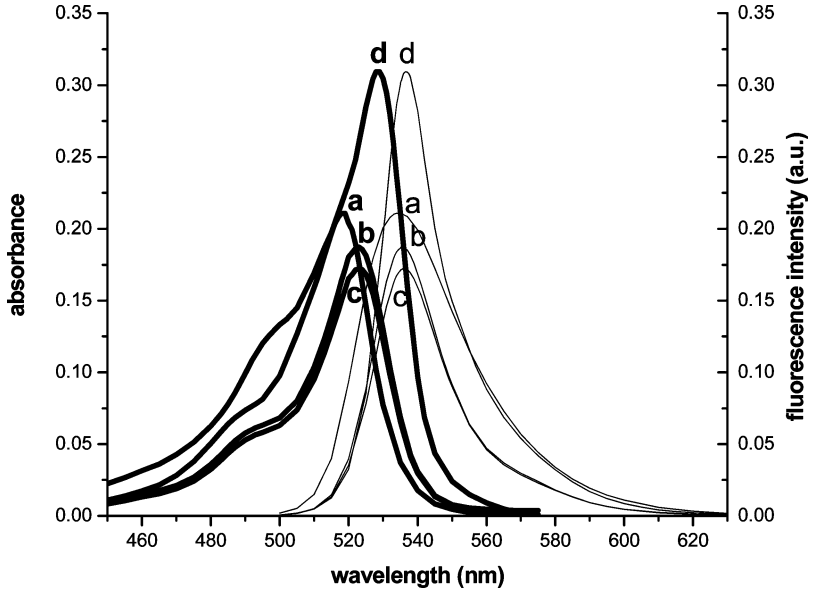

FIGURE 2. Absorption and fluorescence spectra of the PM dyes **1**−**4** in ethanol. Thick and thin lines illustrate absorption and fluorescence spectra, respectively. The spectra of different dyes are represented as (a) dye **1**, (b) dye **2**, (c) dye **3**, and (d) dye **4**.

crowding at the C-8 position of the PM moiety would retard the reaction with $^1O_2$. With this aim, we synthesized three PM567 congeners, **2**−**4** (Scheme 1), following a standard protocol. Given that the pentamethyl-2,6-diethyl PM moiety is known to show remarkably low T−T absorption,[3b] we expected that a structural change at C-8 would not alter the lasing characteristics of the PM dyes, but might increase their photostability.

Each of these compounds possesses a sterically bulky aryl group at the C-8 position of the PM moiety. Among these, the dyes **2** and **3** are known,[8] while **4** is reported for the first time. It is worth mentioning that the conversion of **7** to **8** can be carried out more efficiently with $LiAlH_4$ rather than the Wolff−Kishner reduction, generally used for this purpose. In keeping, compound **8** turned into a thick blackish liquid. Hence we used it immediately for the subsequent steps, carried out in one pot.

Photophysical Characteristics. The photophysical parameters (longest wavelength absorption maxima (λ_{abs}), emission maxima (λ_{em}), and fluorescence quantum yields (Φ_{fl})) of the dyes **2**−**4** relative to those of dye **1** in different polar protic and aprotic solvents are presented in Table 1. Although the absorption and fluorescence spectra of the dyes **1**−**4** were recorded in different solvents, only those obtained in ethanol are shown in Figure 2.

The PM dyes **1**−**4** in ethanol had intense S_0 to S_1 absorption bands at 518−528 nm, each with a small fwhm that is characteristic of the cyanine type of chromophores. Such dyes are found to be of interest as optimizing chromophores for organic photorefractive materials. The spectral properties of the BODIPY chromophore had an exceptionally weak influence from the solvent polarity. The shapes of the absorption spectra of the dyes **2**−**4** were similar to that of **1**, but the maxima were bathochromically shifted by 5−8 nm. Among the dyes, compound **4** showed sharper and stronger absorption and emission spectra, reflecting a significantly high polarizability of the dye chromophore due to the increased π electron cloud.

TABLE 1. Photophysical Parameters of the Dyes 1−4 in Different Solvents

dye	solvent	λ_{abs} (±0.2 nm)	λ_{em} (±0.3 nm)	Φ_{fl}[a]
dye **1**	methanol	517.0	533.0	0.91[b]
	ethyl acetate	517.0	533.0	0.80[b]
	TFE	518.0	533.1	0.97[b]
	ethanol	518.0	534.2	0.84[b]
dye **2**	methanol	522.0	535.1	0.89
	ethyl acetate	522.0	535.6	0.79
	TFE	521.0	534.5	0.95
	ethanol	523.1	536.3	0.78
dye **3**	methanol	522.0	535.4	0.88
	ethyl acetate	522.0	533.6	0.77
	TFE	522.0	535.6	0.92
	ethanol	524.4	535.4	0.76
dye **4**	methanol	527.0	535.5	1.03
	ethyl acetate	527.0	535.4	0.86
	TFE	528.0	536.1	1.09
	ethanol	528.0	536.5	0.85

[a] The fluorescence of the dyes **1**−**4** were measured at O.D. 0.1 at excitation wavelength 490 nm. The fluorescence quantum yields of the dyes **2**−**4** refer relative to that of the dye **1**. [b]The reported[8] data of **1** are presented for comparison.

The fluorescence spectra of the dyes were also identical throughout the series and entirely consistent with fluorescence from the PM subunit.[9] The spectra were almost mirror images of the respective absorption spectra, with minimum energy loss. However, compared to the λ_{abs}, the bathochromic shifts in the fluorescence maxima of **2**−**4** from that of **1** were less (1−3 nm). These results confirmed the insignificant effect of the introduction of the 8-aryl group on the photophysical properties of the PM dyes.[9] Compared to the dye **1**, the relative fluorescence quantum yields (Φ_{fl}) of **2** and **3** were slightly less in all the solvents, while that of **4** was significantly more. The dyes **2**−**4** showed maximum Φ_{fl} in trifluoroethanol (TFE) in which the dye **1** also had maximum fluorescence quantum yield. The dye **4** showed almost the same fluorescence quantum yield as that of **1**, although it was reduced in **2** and **3**.

(8) Lopez, A. F.; Lopez, A. T.; Lopez, A. I.; Garcia-Moreno, I.; Costella, A.; Sastre, R.; Amat-Guerri, F. *Chem. Phys. Lett*. **1999**, *299*, 315−321.

(9) Lo'pez Arbeloa, F.; Bañuelos, J.; Martinez, V.; Arbeloa, T.; Lo'pez, Arbeloa, I. *Int. Rev. Phys. Chem*. **2005**, *24*, 339−374.

TABLE 2. Photophysical and Lasing Parameters of the Dyes 1−4 and Rh6G in Ethanol

dye	λ_{abs} (±0.2 nm)	$\epsilon_{max} \times 10^{-4}$ (M^{-1} cm^{-1})[a]	λ_{fl} (±0.3 nm)	Φ_{fl}[b]	τ (±0.05 ns)[c]	% η (±1.0)[d]	$k_r \times 10^{-8}$ (s^{-1})[e]
dye **1**	518.0	7.1	534.2	0.84	6.59	47.4	1.27
dye **2**	523.1	5.8	536.3	0.78	5.84	36.8	1.34
dye **3**	524.4	6.3	535.4	0.76	5.51	37.2	1.38
dye **4**	528.0	10.4	536.5	0.85	6.98	45.7	1.22
Rh6G	530.0	9.7	556.0	0.95	4.50	24.6	2.11

[a] Extinction coefficients at respective λ_{max}. [b]Fluorescence quantum yield. [c]Fluorescence lifetime. [d]Maximum lasing efficiency at optimized concentrations. [e]Radiative rate.

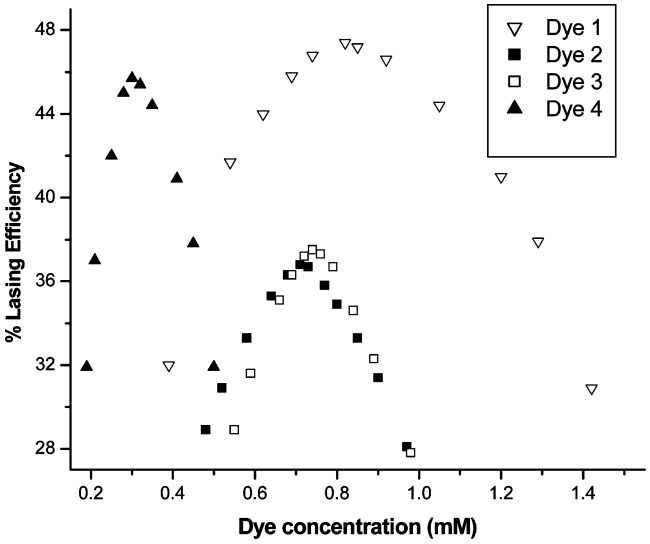

FIGURE 3. Concentration-dependent broad band lasing efficiency of the PM dyes in ethanol.

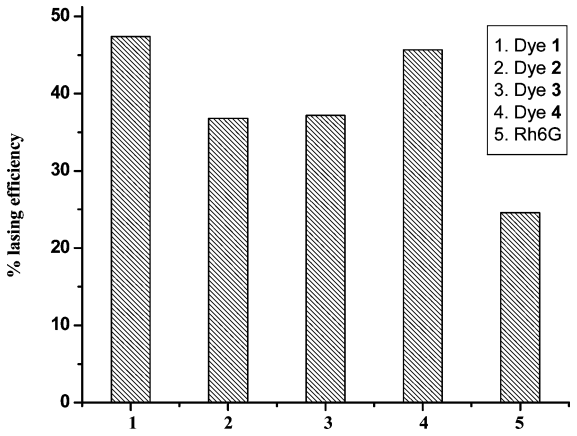

FIGURE 4. Broad band lasing efficiency of the PM dyes **1**−**4** and Rh6G in ethanol, obtained at their respective optimized concentrations. The concentrations of the dyes **1**−**4** and Rh6G were 0.82, 0.71, 0.74, 0.30, and 0.17 mM, respectively.

Some other photophysical parameters of the dyes **1**−**4** as well as rhodamine 6G (Rh6G) in ethanol, which are relevant for their lasing property, are included in Table 2. Comparison of the results of the reference dye **1** and the dyes **2**−**4** revealed interesting features. Incorporation of a phenyl substitution at C-8 (dye **2**) reduced the ϵ_{max} compared to that of **1**, which was compensated by gradual introduction of a +R group (OMe). Thus, the ϵ_{max} of the dye **3** with one OMe group was more than that of **2**, while the ϵ_{max} of **4** possessing three OMe groups exceeded even that of both PM567 and Rh6G. Overall, parameters such as a higher ϵ_{max} and a comparable Φ_{fl} of **4** *vis-à-vis* **1** favored its good lasing efficiency at a lower concentration, compared to **1**. The radiative rates (k_r) of the dyes, calculated using the standard expression $k_r = \Phi_{fl}/\tau$ revealed a maximum value (2.11×10^8) for Rh6G, while those for the PM dyes **1**−**4** were much less ($(1.22-1.38) \times 10^8$).

Lasing Characteristics. The concentration dependent lasing efficiencies of the PM dyes in ethanol (Figure 3) followed an expected pattern, initially increasing with the dye concentration and reaching a maximum before decreasing again. Maximum lasing efficiency values (η) of the dyes at their respective optimum dye concentrations are shown in Figure 4 and also listed in Table 2.

The lasing efficiency of **1**−**4** followed the same pattern as that observed with their respective Φ_{fl} and ϵ_{max} values. This suggested that incorporation of the C-8 aryl group had a similar effect on their respective lasing efficiency. Thus, while the dye **2** showed less efficiency compared to **1**, introduction of one OMe group (in **3**) partially restored the efficiency, which was nearly restored to that of **1** in **4** (three OMe groups). In spite of their smaller fluorescence quantum yields and radiative rates (k_r), all the PM dyes showed substantially higher lasing efficiency than Rh6G. The higher laser efficiencies of the PM dyes may be attributed to their smaller excited-state (singlet−singlet, triplet−triplet) and ground-state absorption cross sections at the laser wavelengths.[10] This is beneficial for power scaling in the master oscillator−power−amplifier design of pulsed dye lasers. Due to steric reasons, the C-8 aryl group in the dyes **2**−**4** would be placed perpendicular to the plane of the PM core (*vide infra*). Further, free rotation of the aryl group would be severely constrained especially in **4** due to the 2,6-methoxyl groups in it. Such a molecular constraint is well-known to enhance fluorescence and, in turn, the lasing efficiency as observed in our studies.

The spatial profile of the lasing output for each dye was circular at the respective maximum lasing efficiency. This would ensure uniform propagation of the laser light over a longer distance, which is beneficial for different types of laser applications. One of the most striking observations was that the dye **4** (0.30 mM) showed almost equal lasing efficiency as that of **1** (0.82 mM). Besides being beneficial from the point of view of economy, use of a smaller concentration of **4** would also reduce the GSA losses at the laser frequencies, improving its lasing performance. Given that the ratio of the ϵ_{max} values of the dyes **4** and **1** was ∼1.5, the former would have 1.5 times more absorption at a comparable concentration. This partially explains the better laser efficiency of **4** at a lower concentration. In addition, a probable difference in the excited and ground states absorption cross-sections of the **1** and **4** at their respective lasing wavelengths might also contribute to this.

(10) Liang, F.; Zeng, H.; Sun, Z. *J. Opt. Soc. Am. B* **2001**, *18*, 1841−1845.

TABLE 3. Quantum Yield of Photodegradation of the PM Dyes 1−4[a]

dye	concn (M) × 10^4	Φ^1_{pd} × 10^4	Φ^2_{pd} × 10^6	$\Phi^1_{pd}{}^{-1}$ of **2**−**4**/ $\Phi^1_{pd}{}^{-1}$ of **1**	$\Phi^2_{pd}{}^{-1}$ of **2**−**4**/ $\Phi^2_{pd}{}^{-1}$ of **1**
dye **1**	1.4	1.166	16.30		
dye **2**	1.6	0.383	2.73	3.04	5.97
dye **3**	1.5	0.427	5.04	2.73	3.23
dye **4**	1.2	0.585	9.11	1.99	1.79

[a] Different concentrations of the dyes were used to maintain the O.D. values of their solution at ∼1 at their respective λ_{max}.

Photostability Characteristics. The quantum yields of photodegradation of the dyes **1**−**4** at different concentrations, measured in air-equilibrated ethanol solution without or with 100 mM DABCO (Φ^1_{pd} and Φ^2_{pd}, respectively) are shown in Table 3. The enhancement in photostability ($\Phi_{pd}{}^{-1}$) of the PM dyes **2**−**4** in ethanol, compared to that of **1** under the above conditions, are shown in columns 5 and 6, respectively, of the same table.

All the dyes **2**−**4** showed higher photostability than **1** (Table 3, columns 5 and 6), which was more in the presence of the singlet oxygen quencher, DABCO. The effect of DABCO further confirmed the role of $^1O_2$ in the photodegradation of the PM dyes.

Among the dyes, **2** showed the highest photostability, which was gradually reduced on increasing the numbers of the OMe substituents in the phenyl ring (dyes **3** and **4**). However, even then, the photostability of **4** was double that of **1**, under irradiation by a 532 nm pump. The effect of DABCO (100 mM) on the photostablities of the dyes was different, being most pronounced for **2** followed by **3**. With **4**, DABCO had a marginal effect, suggesting the formation of an insignificant amount of $^1O_2$ during its photoexcitation. In separate experiments, we have also confirmed the dye degradation by HPTLC analyses of the individual dyes after irradiation with the 532 nm pump for 20 min (see Supporting Information, Table S1). To confirm that the $^1O_2$ or other active oxygen species (produced during photoexcitaion of the PM dyes) reacts primarily at the olefinic site and not at the aryl moiety at C-8, we also measured the reduction potentials of the compounds **1** and **4** using cyclic voltammetry (see Supporting Information, Figure S2 and Figure S3). The lower reduction potential of the dye **4** (−1.236 V) than that of the dye **1** (−1.363 V) confirmed that the photooxidation of the PM dyes occurs overwhelmingly at the olefin function. We did not observe any change in shape of the longest wavelength absorption band (S_0-S_1) of the dye solutions, except for the decrease in peak heights, during photoexposure. This was expected considering that the degradation of the dyes at the olefinic site produces nonfluorescent products, which would not interfere with the spectral measurements of the dye solutions.

Characterization of Photodegradation Products. The HPLC and LCMS analyses of the photodegradation products of the PM dyes revealed that the process followed an identical pathway irrespective of the nature of the C-8 substituent in them. All the dyes gave three major common products as revealed from HPLC (see Supporting Information, Figure S4 and S5). One of the products (RT 7.02 min, M^+ 187) was identified as **9**, while the other (RT 7.21 min, M^+ 324) was attributed to **10**. Both these products are formed by 1,2-cycloaddition of $^1O_2$ at the C-8 olefinic site of the PM dye structure followed by suitable cleavage as shown in Figure 5. This is consistent with our electrochemical results of the dyes and also that observed earlier.[6c]

TABLE 4. Net Charges (Mulliken) on Different Atoms of the Dyes 1−4 at Their Respective Optimized Ground State Geometries, Calculated by *ab Initio* Hartree−Fock (6-31G)**

dye	C-1	C-2	C-3	N-3′	B-4	C-8	C-8′	C-9
dye **1**	+0.03	−0.15	+0.35	−0.80	+1.13	+0.08	+0.18	−0.35
dye **2**	+0.03	−0.16	+0.36	−0.80	+1.13	+0.02	+0.21	−0.06
dye **3**	+0.03	−0.16	+0.37	−0.81	+1.15	+0.02	+0.21	−0.09
dye **4**	+0.05	−0.17	+0.37	−0.82	+1.16	+0.05	+0.22	−0.20

TABLE 5. Calculated Absorption Parameters of 1−4 Using CIS and TDDFT Methods

	CIS			TDDFT		
dye	$E_{S_0\rightarrow S_1}$ (eV)	λ_{abs} (nm)	f	$E_{S_0\rightarrow S_1}$ (eV)	λ_{abs} (nm)	f
dye **1**	3.434	361.0	0.9666	2.815	440.0	0.2627
dye **2**	3.400	364.7	0.9685	2.774	447.0	0.2088
dye **3**	3.378	367.0	0.9357	2.774	447.0	0.2105
dye **4**	3.338	371.4	0.8788	2.769	447.6	0.2375

The additional common photodegraded product (RT 6.73 min, M^+ 304) was assigned the structure **11** and produced by direct scission of the C-8 substituents (Figure 5). Formation of additional products **12a** (M^+ 94), **12b** (M^+ 124), and **12c** (M^+ 184) from **2**−**4**, respectively, which account for the C-8 aromatic substituents also confirmed the direct photolysis of the dyes.

Theoretical Interpretations. The PM dyes **1**−**4** possess a compact chromophore with large values of the integrated absorption, which can be used to explore the electronic structure of BODIPY by means of semiempirical calculations.[11] In our studies we analyzed the absorption characteristics and reactivity of the PM dyes **1**−**4** with $^1O_2$ by extensive theoretical calculations to explain their lasing efficiency and photostability. The *ab initio* MO calculations were carried out using the better features of both Spartan'02 (Unix), Wavefunction, Inc. (USA), 2001 and Gaussian 03 (Unix), Gaussview-3, Gaussian, Inc. (USA), 2003 softwares. The geometries of the dyes were optimized in their respective ground states by the *ab initio* Hartree−Fock method and 6-31G** basis set.

Analysis of the Mulliken charge distribution (Table 4) over the atoms of the PM chromophore unit did not show much variation in the electron densities at different atoms, except at C-9. Changing of the C-8 methyl substituent of **1** to the phenyl group led to an abrupt decrease in the electron density at C-9 in **2**. This was, however, compensated by a gradual introduction of the electron donating OMe groups in the dyes **3** and **4**.

The change in electron density at C-9 appeared to have a correlation with the change in broad band lasing efficiency of the PM dyes. The boron atom plays a crucial role in bridging the two pyrromethene units in the PM dyes, ensuring extended conjugation that is essential for their lasing property. The Lewis acidity of boron coupled with its size compatibility with the pyrrole nitrogen atoms is responsible for this. Evidently, a higher electron density at C-9 in **4**, as found in our theoretical calculations, would facilitate the extended conjugation explaining its superior lasing efficiency.

The absorption parameters such as excitation energies ($E_{S_0\rightarrow S_1}$) and oscillator strength (*f*) of the dyes were calculated at their respective ground state geometries with the help of a singles excitation method, CIS. The trend of bathochromic shifts in the absorption maxima of **1**−**4**, observed by experiments, was also

(11) Bergström, F.; Mikhalyov, I.; Hägglöf, P.; Wortmann, R.; Ny, T.; Johansson, L. B.-Å. *J. Am. Chem. Soc*. **2002**, *124*, 196−204.

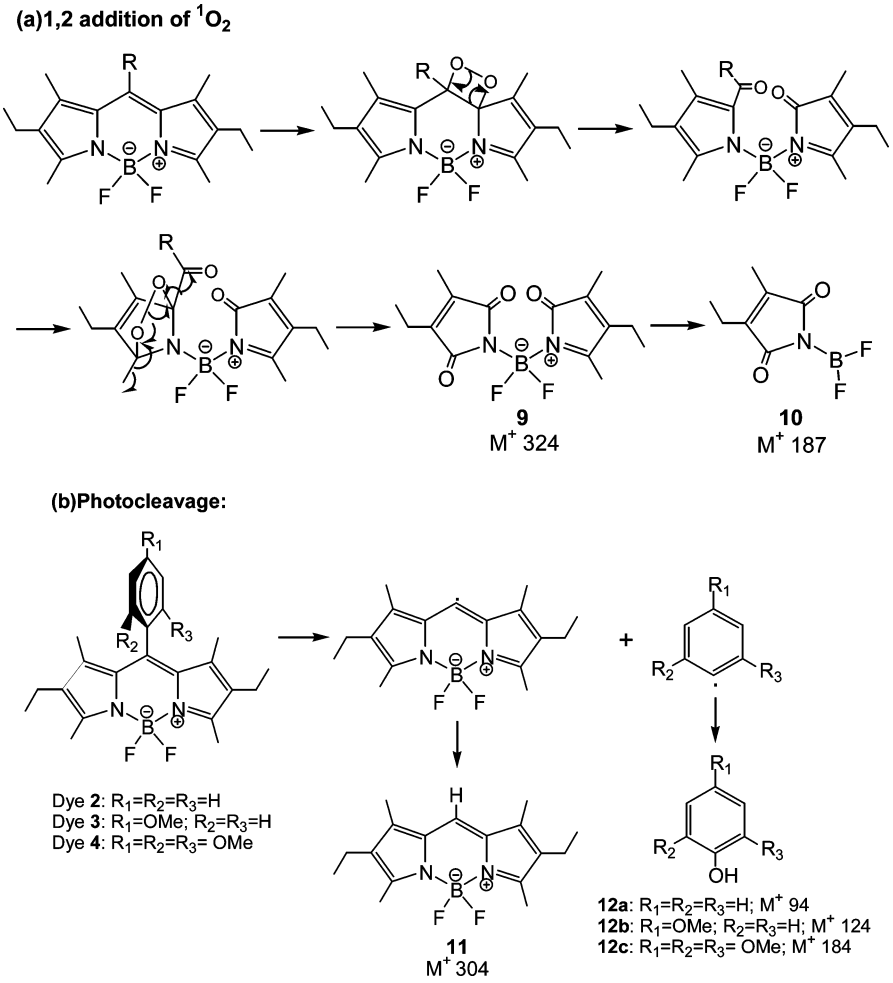

FIGURE 5. Photodegradation products of the PM dyes **1**−**4**.

TABLE 6. Ab Initio Calculated Molecular Parameters of the Dyes 1−4, 11, and 13

molecular paramaters	dye **1**	dye **2**	dye **3**	dye **4**	**11**	**13**
E-HOMO (eV)	−6.8022	−6.7374	−6.7158	−6.7123	−6.8092	−8.2127
E-LUMO (eV)	+1.0171	+1.0005	+0.9988	+0.9468	+0.9172	+4.7577
band gap(eV)	+7.8193	+7.7379	+7.7145	+7.6590	+7.7264	+12.9703
μ_0 (debye)	+4.5544	+4.8522	+5.8935	+5.0115	+4.0618	+0.0000
μ (S_1, debye)	+4.5750	+4.9276	+5.9608	+5.0260	+4.0875	+0.0017

indicated by the CIS calculation (from 361 to 371 nm) (Table 5). The coefficients of leading configurations (HOMO → LUMO values for all the dyes ∼0.9) indicated that, in all the dyes, the CIS excited states arise from HOMO → LUMO transitions. Compared to the experimental results, calculation by the CIS method furnished shorter λ_{max} values. However, this is due to the shortcoming of the theoretical method, as reported earlier.[12]

A better program for calculating the transition energies is the TDDFT method, employing an LSDA exchange-correlation potential within the DFT model. Hence this was also used taking the same basis set to calculate the transition energies. Among the various available potentials and hybrid functionals (LSDA, B3PW91, B3LYP, MPW1PW91, PBE1PBE), the LSDA performed best. The blue-shifted absorptions (by CIS) were corrected to a large extent but not completely by this program (Table 5). The effect of solvent molecules was not considered in the calculations, which might partially explain the differences between the calculated and experimental values. The ZINDO method, which is more commendable for this purpose, could not be availed because it lacks parameters for boron within Gaussian03.

Our calculations of the molecular parameters revealed a minimum change of the dipole moments of the S_o and S_1 states of all the dyes explaining[13a,b] the weak solvatochromism. The calculated dipole moments of the dyes **2**−**4** both in the ground (μ_0), excited singlet (μ_{S1}) states were more than that of **1** (Table 6), suggesting better polarizability of the chromophore and associated higher lasing efficiency of the former dyes, as

(12) Stratmann, R. E.; Scuseria, G. E. *J. Chem. Phys.* **1998**, *109*, 8218−8224.

(13) (a) Reichhardt, W. *Solvents and solvents effects in organic chemistry*; VCH: Weinheim, 1988. (b) Liptay, W. *Dipole Moments and Polarizabilities of Molecules in Excited Electronic State*; Lim, E. C., Ed.; Academic Press: New York, 1974; Vol. 1, pp 129−229.

TABLE 7. Ab Initio Calculated HOMO and LUMO Energies in $^1O_2$ and $^3O_2$

	RHF-$^1O_2$		UHF-$^3O_2$			
molecular orbital	HOMO	LUMO	α-HOMO	α-LUMO	β-HOMO	β-LUMO
Hartree−Fock ab initio (6-31G**) orbital energy eigenvalues (eV)	−12.2715	1.3328	−14.564	13.0781	−16.2102	3.5947

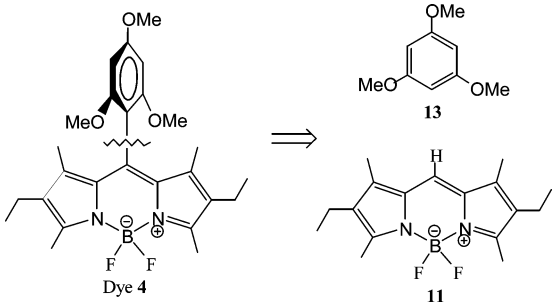

FIGURE 6. Chemical structures of the PM dyes **11** and **13**.

observed by experiments. Admittedly, the experimental results did not exactly match with the theoretical predictions but provided a rationale to explain the better lasing efficiency of the dye **4**.

Considering the role of $^1O_2$ in the photodegradation of the PM dyes, the increase in their photostability can be attributed to their reduced ability to react and/or generate $^1O_2$. The reactivity of the dyes toward $^1O_2$ can be governed by steric and/or electronic factors. Comparison of the HOMO and LUMO energies of the dyes (Table 6) and $^1O_2$ (Table 7) revealed that the reaction between the HOMO of dyes and LUMO of $^1O_2$ is more favored than that between the LUMO of the dyes and HOMO of $^1O_2$. Further, the band gap between HOMO−LUMO of the dyes gradually decreased along the sequence, dye **1** to dye **4** (Table 6). Thus, considering the electronic factor alone, the theoretical calculation predicted the relative reaction probability of $^1O_2$ with the dyes as **1** < **2**< **3** < **4**.

Regarding the photodecomposition of the compound **4**, the relative reaction probability of its constituent segments, the PM core (**11**) and the aryl moiety (**13**) (Figure 6) with $^1O_2$ was also estimated. The energy gap LUMO ($^1O_2$) − HOMO (**13**) is significantly higher (1.4035 eV) than that of LUMO ($^1O_2$) − HOMO (**11**) (Table 6). This clearly revealed that the photooxidation of **4** would be exclusively at the C-8 olefin function.

The theoretical calculated relative reaction probability of $^1O_2$ with the dyes was in contrast to the experimental results and indicated that the reaction probability might be controlled more significantly by the steric parameters. Calculations based on conformational analysis of the dye chromophores **2**−**4** revealed that the plane containing the aryl groups to be perpendicular with respect to the PM ring, suggesting an insignificant influence of the electronic $\pi-\pi$ resonance interactions between the C-8 aryl group and the PM moiety. This was also corroborated by our experimental results on the photophysical properties of the PM dyes. The structural disposition could be due to the geometrical restrictions imposed by the C-1 and C-7 methyl groups. It was found that the active double bond site of the PM moiety in **2** and **3** is spatially crowded from both the sides by the H-2 and/or H-6 atoms of the aryl groups in the dyes. The crowding would be more severe in the case of **4**, possessing the bulkier OMe group in both these positions of the phenyl moiety, reducing the probability of its reaction with $^1O_2$ further.

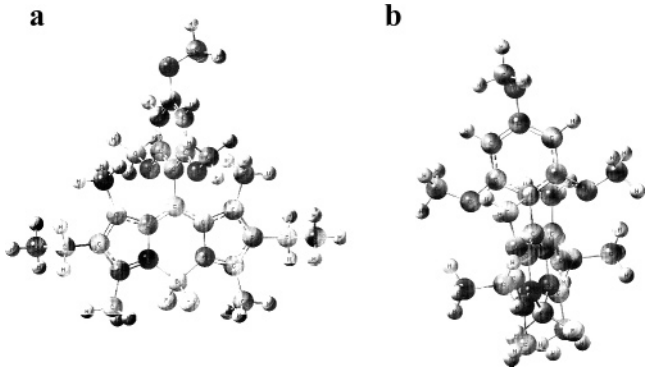

FIGURE 7. (a) XY and (b) XZ views of the energy minimized structure of **4**, as revealed from the Gaussian-03 calculation.

As a representative example, the geometry of the ground state of **4**, derived from *ab initio* calculations, is illustrated in Figure 7.

The steric energies of the PM dyes, estimated from the molecular mechanics MM2 calculation (Table 8), also revealed maximum steric energy of **4**, which was >10 kcal/mol than that of **1**. Due to the presence of the planer unsubstituted phenyl group in **2**, the steric interaction between the C-8 substituent and the C-1 and C-7 methyl groups of the PM molecule is expected to be minimum accounting for its lowest steric energy. However, even then the H-2 and/or H-6 atoms of the C-8 phenyl ring would cover both the faces of the reaction site (double bond) of the dye molecules, hindering their reaction with $^1O_2$. Overall, from a steric perspective the relative probability of the reaction with $^1O_2$ would be dye **1** > dye **2** ≈ dye **3** ≫ dye **4**. This more or less correlated with our experimental results, which showed the photodegradation trend as dye **1** > dye **4** > dye **3** ≈ dye **2**. The comparative lower stability of **4** *vis-à-vis* that of **2** and **3** indicates a greater contribution of the electronic factor for the former, as anticipated. Evidently, the electronic factor contributes significantly with compound **4**. This was expected considering the higher calculated electron densities at its C-8 and C-9 positions (Table 4).

With regard to the generation of $^1O_2$ by the PM dyes, the calculated triplet excitation energies (E_T) revealed maximum (25.48 kcal/mol) and minimum (22.16 kcal/mol) values, respectively, for the dyes **1** and **4** (Table 9). It is known that molecular oxygen has a ground triplet state ($^3\Sigma$) and an excited singlet state comprising two very low-lying states ($^1\Delta$ and $^1\Sigma$) with T−S excitation energies as 22.50 kcal/mol and 37.5 kcal/mol,[14] respectively. Thus, sensitizers possessing excitation energies ∼23 kcal/mol may be quenched via energy transfer to produce $^1O_2$ in its $^1\Delta$ state according to:

$$\text{Sens}^* + {}^3O_2({}^3\Sigma) \rightarrow \text{Sens} + {}^1O_2({}^1\Delta)$$

In consideration of the E_T values of the dyes, the yield of $^1O_2$ generation would gradually fall from dye **1** to dye **4**. It is apparent that PM567 can very well generate $^1O_2$, which, in turn,

TABLE 8. Steric Energies of the PM Dyes 1−4

dye	1	2	3	4
steric energies (kcal/mol)	19.3909	13.0432	18.5264	29.9860

TABLE 9. Ab Initio Calculated Energies of the Singlet/RHF and Triplet/UHF States

dye	energy of $^1S_0$, E_{RHF} (au)	energy of $^3T_1$, E_{UHF} (au)	$E_T = {}^3T_1 - {}^1S_0$ (kcal/mol)
dye **1**	−1028.883 301 35	−1028.842 699 36	25.48
dye **2**	−1219.400 211 71	−1219.364 167 78	22.62
dye **3**	−1333.280 880 29	−1333.244 973 94	22.53
dye **4**	−1561.044 900 43	−1561.009 581 82	22.16

can react with the $^1S_0$ state of the dye leading to its degradation. Since the E_T value of **4** was marginally less than that of molecular oxygen, it would generate a minimum amount of $^1O_2$, although the possibility of $^1O_2$ generation by **4** cannot be completely excluded. Thus, the relative $^1O_2$ generation capacities of the dyes would be dye **1** > dye **2** > dye **3** > dye **4**. The marginal effect of DABCO in the photodegradation of **4** was consistent with calculated values.

Overall, the better photostability of the PM dyes **2**−**4** *vis-à-vis* **1** can be attributed to the combined effects of lesser capacity to generate $^1O_2$ and probability to react with the $^1O_2$. Among the controlling factors for the photostability of the dyes, the contribution of steric hindrance outweighs the electronic factor favoring lower reactivities of the dyes **2**−**4**, especially dye **4** with $^1O_2$. In addition, the relative triplet state energies of the dyes and excitation energy of $^1O_2$ predict formation of a minimum amount of $^1O_2$ with **4**. All these factors ultimately make the dye **4** two times more photostable than dye **1**.

Conclusions

Overall, we have developed a new pyrromethene laser dye **4** with improved lasing characteristics and photochemical stability by a rational design. The synthesis is based on replacing the C-8 methyl group with a suitable aryl group following a convenient protocol. Considering the prohibitively high cost[5a] of the PM dyes, the ease of preparation of the new dyes would be very attractive for a wider availability and application. Incorporation of a C-8 aryl group increased the photostability of the PM molecules. It was shown that the associated reduction in fluorescence and lasing efficiencies can be efficiently modulated by introducing suitable electron donating groups. Our theoretical calculations on the electron densities, energy levels (HOMO, LUMO), and steric energies of the dye, as well as, singlet oxygen generation capacity provided a rationale to explain most of the experimental observations. The study provided possible future directions to improve the design of highly efficient PM dye molecules in terms of higher photochemical stability for their applications in liquid dye lasers.

Experimental Section

Ethyl 4-Acetyl-3,5-dimethyl-1*H*-pyrrole-2-carboxylate (6). To a stirred cooled (0 °C) solution of ethyl acetoacetate (4.9 g, 0.038 mol) in acetic acid (10 mL) was added a cold solution of sodium nitrite (2.8 g, 0.041 mol) in H_2O (10 mL). After stirring the mixture for 24 h at 25 °C, acetyl acetone (3.8 g, 0.038 mol) and zinc dust (5.3 g) were added, and the mixture was stirred at 60 °C for 1 h. The mixture was brought to room temperature and extracted with $CHCl_3$. Concentration of the extract in vacuo followed by crystallization from $CHCl_3$ gave **6** as a white solid (6.35 g, 80%). Mp: 142 °C (lit.[15] mp: 143−144 °C); IR: 3302, 1678, 1646 cm^{-1}; ^1H NMR: δ 1.36 (t, J = 7.1 Hz, 3H), 2.43 (s, 3H), 2.51 (s, 3H), 2.57 (s, 3H), 4.34 (q, J = 7.1 Hz, 2H), 9.41 (broad s, 1H, NH); ^{13}C NMR: δ 12.5, 14.1, 14.6, 30.9, 60.2, 117.8, 123.1, 129.3, 138.9, 162.0, 195.4; MS (*m*/*z*): 209 (M^+).

2,4-Dimethyl-3-acetyl-1*H*-pyrrole (7). A mixture of **6** (3.0 g, 0.014 mol) and KOH (1.5 g, 0.027 mol) in ethylene glycol (10 mL) was heated at 160 °C for 4 h. After cooling, the mixture was extracted with $CHCl_3$, and the extract was washed with water and brine and dried. Removal of solvent gave pure **7** as a white solid (1.86 g, 97%). Mp: 96 °C; IR: 3300, 1680 cm^{-1}; ^1H NMR: δ 2.26 (s, 3H), 2.43 (s, 3H), 2.50 (s, 3H), 6.36 (s, 1H), 8.52 (broad s 1H, NH); ^{13}C NMR: δ 13.7, 15.2, 30.7, 115.0, 120.5, 120.7, 136.2, 195.9; MS (*m*/*z*): 137 (M^+). Anal. Calcd for $C_8H_{11}NO$: C, 70.04; H, 8.08; N, 10.21. Found: C, 70.10; H, 8.02; N, 10.17.

2,4-Dimethyl-3-ethyl-1*H*-pyrrole (8). To a stirred suspension of $LiAlH_4$ (0.333 g, 8.76 mmol) in dry THF (20 mL) was added **7** (1.0 g, 7.30 mmol) in THF (10 mL). The mixture was refluxed for 4.5 h and brought to room temperature, and the excess hydride was decomposed with aqueous saturated Na_2SO_4. The mixture was extracted with chloroform, and the extract was concentrated in vacuo. The residue was subjected to column chromatography (neutral Al_2O_3, hexane−EtOAc) furnishing **8** as a brown liquid (0.673 g, 75%). IR: 3377, 1689, 1644 cm^{-1}; ^1H NMR: δ 1.23 (t, 3H, J = 7.4 Hz), 2.18 (s, 3H), 2.28 (s, 3H), 2.54 (q, J = 7.4 Hz, 2H), 6.48 (s, 1H), 7.51 (broad s, 1H, NH); ^{13}C NMR: δ 10.1, 10.9, 15.5, 17.3, 112.8, 117.4, 120.1, 123.1; MS (*m*/*z*): 123 (M^+).

2,6-Diethyl-4,4-difluoro-1,3,5,7-tetramethyl-8-phenyl-4-bora-3a,4a-diaza-s-indecene (2). A mixture of **8** (0.450 g, 3.7 mmol), benzaldehyde (0.196 g, 1.85 mmol), and *p*-toluenesulphonic acid (0.015 g) in dry CH_2Cl_2 was stirred at room temperature for 24 h. DDQ (0.420 mg, 1.85 mmol) was added to the resulting deep red solution, and stirring continued for 4 h. The mixture was treated with triethylamine (0.5 mL) and stirred for another hour. Finally, $BF_3{\cdot}Et_2O$ (0.762 mL, 4.6 mmol) was added to the mixture in portions during 4 h, and the solution stirred at room temperature overnight. The resulting dark mixture was washed with aqueous saturated $NaHCO_3$, water, and brine and dried. Removal of solvent in vacuo followed by column chromatography of the residue (silica gel, hexane−EtOAc) furnished **2** (0.175 g, 24.9%), which was recrystallized from hexane to afford orange needles. Mp: 184−185 °C (lit.[1g] mp 185−186 °C); ^1H NMR: δ 0.97 (t, J = 7.6 Hz, 6H), 1.26 (s, 6H), 2.27 (q, J = 7.6 Hz, 4H), 2.52 (s, 6H), 7.25−7.29 (m, 2H), 7.45−7.48 (m, 3H); ^{13}C NMR: δ 11.6, 12.5, 14.6, 17.1, 128.3, 128.7, 129.0, 130.8, 132.7, 135.8, 138.4, 140.2, 153.7; MS (*m*/*z*): 380 (M^+).

2,6-Diethyl-4,4-difluoro-1,3,5,7-tetramethyl-8-(4′-methoxyphenyl)-4-bora-3a,4a-diaza-s-indecene (3) and 2,6-Diethyl-4,4-difluoro-1,3,5,7-tetramethyl-8-(2′,4′,6′-trimethoxyphenyl)-4-bora-3a,4a-diaza-s-indecene (4). Following the same procedure, the dyes **3** (0.094 g, 28%) and **4** (0.85 g, 22%) were prepared from **8** using 4-methoxybenzaldehyde and 2,4,6-trimethoxybenzaldehyde, respectively.

3.[10] Mp: 192 °C; ^1H NMR: δ 0.97 (t, J = 7.4 Hz, 6H), 1.32 (s, 6H), 2.29 (q, J = 7.4 Hz, 4H), 2.52 (s, 6H), 3.87(s, 3H), 7.0 (d, J = 8.6 Hz, 2H), 7.14 (d, J = 8.6 Hz, 2H); ^{13}CNMR: δ 11.8, 12.5, 14.6, 17.1, 55.3, 114.4, 127.9, 129.5, 131.2, 132.6, 138.4, 153.5, 160.0; MS (*m*/*z*): 410 (M^+).

4. Mp: 157 °C; ^1H NMR: δ 1.05 (t, 6H, J = 7.6 Hz), 1.57 (s, 6H), 2.15 (s, 6H), 2.37 (q, 4H, J = 7.6 Hz), 2.48 (s, 6H), 3.76 (s, 3H), 6.08 (s, 1H), 6.93 (s, 1H); ^{13}CNMR: δ 9.4, 12.5, 14.6, 17.3, 55.3, 92.9, 118.5, 131.6, 132.4, 136.6, 154.7,161.5; MS (*m*/*z*): 470 (M^+).

(14) Reference 4d, p 354.

(15) Shrout, D. P.; Lightner, D. A. *Synthesis* **1990**, 1062−1065.

Anal. Calcd for $C_{26}H_{33}BF_2N_2O_3$: C, 66.39; H, 7.07; N, 5.96. Found: C, 66.44; H, 7.14; N, 5.91.

Photophysical Studies. The absorption and emission spectra of the dyes ($\sim 10^{-6}$ M) in various solvents were measured using a 1 cm quartz cuvette. The fluorescence quantum yields (Φ_{fl}) of the dyes **2**−**4** relative to that of the reference dye **1**[8] and the molar extinction coefficients (ϵ_{max}) were determined in ethanol. The excited state (S_1) lifetimes of **2**−**4** in ethanol were determined by the time-resolved fluorescence measurements, carried out using an LED based time-correlated single-photon-counting (TCSPC) spectrometer. The fluorescence decays were measured with a 490 nm LED (1 MHz) excitation source and a TBX4 detection module coupled with a special Hamamatsu PMT. The instrument response function was 1.2 ns at fwhm. Following deconvolution analysis of the fluorescence decays, the time resolution of the present setup was ∼50 ps. All the measurements were carried out at ambient room temperature (298 ± 1 K) using a microprocessor based temperature controller.

Lasing Studies. The comparative lasing efficiencies of the dye solutions were measured using a broad-band dye laser setup that was transversely pumped by the second harmonic (at 532 nm) of a Q-switched Nd:YAG laser, at a repetition rate of 10 Hz with ∼5.8 mJ pulse energy and ∼6 ns fwhm pulses. A schematic of the dye laser set up is shown as Supporting Information (Figure S1). To reduce the pulse to pulse fluctuations, the Nd:YAG laser was operated at a higher pulse energy (∼100 mJ) by adjusting the Q-switch timing appropriately. The pump energy was attenuated by a combination of a half-wave and a polarizer plate. The pump beam was divided into two parts by a 50% beam splitter. One part was routed to the dye cell by a mirror, while the other part was routed to a power meter for measuring the average power. The individual dye solutions were taken in a 1 cm quartz dye cell (optical path ∼6 mm along the dye laser axis) that was carefully sealed by a stopcock to avoid solvent evaporation during experiments. The dye cell was placed between a high reflectivity (>99%) mirror and an output coupler (4% reflectivity, wedge angle ∼1°), and the dye solutions were continuously stirred by a Teflon coated magnetic bar to avoid local heating due to the pump beam. The dye cells were suitably tilted along the laser axis to avoid dye cell window lasing along the resonator axis. The pump beam (diameter ∼6 mm) was focused by a cylindrical lens (focal length ∼15 mm) to form a line image in the dye solutions. The broad band lasing efficiency of each dye solution was determined as a function of the dye concentrations, keeping other parameters, including alignment of the cavity, unchanged. For this, different concentrations of the dyes **2**−**4**, and the reference dyes, **1** and Rh6G in ethanol, were used keeping the optical density at 1−5 at the pump wavelength (532 nm).

Photostability Studies. The rate of photodegradation of the dyes in ethanol was experimentally measured under irradiation from the 532 nm output of a pulsed Nd:YAG laser. The measurements were carried out using 2 mL of the dye solutions in the absence[4b] of lasing conditions, by removing the cavity mirrors. The pump beam was directly incident on the dye solution, taken in the same dye cell, without any focusing lens. In each case, the dye concentration was adjusted such that the entire pump energy (∼6 mJ/pulse) was absorbed by the dye solution over the irradiation period (∼1.5 h). The change in absorbances of the dye solutions were periodically measured using an absorption spectrophotometer to monitor the progressive decrease in the dye concentration. The average power of the incident pump radiation was measured by a power meter, and quantum yields of dye photodegradation[16] were calculated.

Photodegradation Products Analysis. 2 mL of ethanol solution of each dye were irradiated by the 532 nm output of a pulsed Nd:YAG laser (pump energy ∼6 mJ/pulse) in the absence[4b] of lasing conditions, by removing the cavity mirrors. The pump beam was directly incident on the dye solution, taken in the same dye cell, without any focusing lens. The dye solutions were irradiated until all the dye molecules degraded. Then HPLC and LCMS were done with photodegradated dye solutions using a C18 column (250 mm × 4.6 mm, 5μ) and an acetonitrile−H_2O (80:20) mixture as solvent at a flow rate of 0.5 mL/min. The products were detected at 254 nm.

Electrochemical Studies. Cyclic voltammetry studies were carried out in deoxygenated ethanol containing 0.1 M tetraethylammonium iodide as the supporting electrolyte. The reduction potentials of the compounds **1** and **4** were measured against a standard Calomel electrode as reference at a scan rate of 100 mV s^{-1}.

Acknowledgment. We thank A. K. Satpati of ACD, BARC for his help in electrochemistry experiments.

Supporting Information Available: ^1H and ^{13}C NMR spectra of the intermediates and dyes. Schematic diagram of the Nd:YAG laser setup used for the lasing experiments. Cyclic voltammogram of dye **1** and **4**. HPLC profile of the photodegradated products of the dye **1** and **4**. HPTLC data for photodegradation of the dyes and configuration coefficients of the dyes (S_1 state) as calculated by the TDDFT method. Computational Data. These materials are available free of charge via the Internet at http://pubs.acs.org.

JO702346S

(16) Sinha, S.; Ray, A. K.; Kundu, S.; Sasikumar, S.; Nair, S. K. S.; Dasgupta, K. *Appl. Phys. B* **2001**, *72*, 617−621.